

Coarsening to chaos-stabilized fronts

Ka-Fai Poon* and Ralf W. Wittenberg†

Department of Mathematics, Simon Fraser University, Burnaby, British Columbia, Canada V5A 1S6

(Received 5 May 2010; revised manuscript received 19 November 2010; published 27 January 2011)

We investigate a model for pattern formation in the presence of Galilean symmetry proposed by Matthews and Cox [Phys. Rev. E **62**, R1473 (2000)], which has the form of coupled generalized Burgers- and Ginzburg-Landau-type equations. With only the system size L as a parameter, we find distinct “small- L ” and “large- L ” regimes exhibiting clear differences in their dynamics and scaling behavior. The long-time statistically stationary state contains a single L -dependent front, stabilized globally by spatiotemporally chaotic dynamics confined away from the front. For sufficiently large domains, the transient dynamics include a state consisting of several viscous shocklike structures that coarsens gradually, before collapsing to a single front when one front absorbs the others.

DOI: [10.1103/PhysRevE.83.016211](https://doi.org/10.1103/PhysRevE.83.016211)

PACS number(s): 05.45.-a, 02.30.Jr, 47.52.+j, 47.54.-r

I. INTRODUCTION

In the exploration of the rich and diverse range of spatiotemporal dynamics observed in nonlinear, nonequilibrium spatially extended systems, it has proved particularly fruitful to investigate comparatively simple model partial differential equations (PDEs) whose solutions capture the essential features of the phenomena under investigation. Thus Burgers’ equation has been extensively studied for the evolution and statistics of shocks; the Ginzburg-Landau (GL) equation and its generalizations describe the dynamics and stability of modulations of patterned states; and the Kuramoto-Sivashinsky and other models display spatiotemporal chaos [1]. In this paper we discuss a system describing the amplitude evolution for pattern formation with symmetry, which appears to combine features of several of these canonical systems and displays a surprising wealth of behaviors.

We investigate the Matthews-Cox (MC) equations [2]

$$A_T = A + 4A_{XX} - ifA, \quad (1)$$

$$f_T = f_{XX} - |A|_X^2, \quad (2)$$

on a one-dimensional L -periodic domain, where A is complex, f is real, and $f_X \equiv \partial_X f \equiv \partial f / \partial X$ (similarly for the other derivatives). Equations (1)–(2) were initially derived in the context of the Nikolaevskiy PDE

$$u_t + uu_x = -\partial_x^2 [\varepsilon^2 - (1 + \partial_x^2)^2] u. \quad (3)$$

This equation, which was proposed originally to model seismic-wave behavior in viscoelastic media [3] and has subsequently arisen in models of phase dynamics in oscillatory reaction-diffusion systems [4,5] and transverse instabilities of traveling fronts [6], appears to be a canonical model for short-wave pattern formation with reflection symmetry $x \mapsto -x$, $u \mapsto -u$ and Galilean invariance $x \mapsto x - vt$, $u \mapsto u + v$ (v constant) [2,7].

Unlike in more common pattern-forming contexts described at onset by the GL equation, the $\mathcal{O}(\varepsilon)$ stationary rolls in the Nikolaevskiy equation (3) are all unstable for all $\varepsilon > 0$ [2,6,8,9]. Instead, solutions of Eq. (3) exhibit spatiotemporal chaos with strong scale separation [10,11], with coupling between the weakly unstable pattern at wave numbers $k \approx 1$ and the neutrally stable long-wave mode with $k \approx 0$. This suggests the ansatz $u(x,t) \sim \varepsilon^{\alpha_1} A(X,T)e^{ix} + \text{c.c.} + \varepsilon^\beta f(X,T) + \dots$ for the envelopes A and f of the pattern and long-wave modes, respectively, where $X = \varepsilon x$, $T = \varepsilon^2 t$. Matthews and Cox [2] showed that the asymptotically self-consistent scaling as $\varepsilon \rightarrow 0$ is $\alpha_1 = 3/2$, $\beta = 2$, and hence derived Eqs. (1)–(2) from the Nikolaevskiy PDE as the leading-order modulation equations [although there is numerical evidence that the scaling behavior on the attractor of Eq. (3) may be anomalous and insufficiently described by this ansatz [11]].

As pointed out in Ref. [2], the asymptotically leading-order modulation equations for pattern formation with these symmetries generally have the structure of Eqs. (1)–(2) (with at most one free parameter, after rescaling), where we note that the action of the odd reflection symmetry is $X \mapsto -X$, $f \mapsto -f$, $A \mapsto -A^*$, while the Galilean invariance acts on the amplitudes via $X \mapsto X - \varepsilon VT$, $f \mapsto f + V$, $A \mapsto Ae^{iVT}$ (with $v = \varepsilon^2 V$). Beyond the connection with Eq. (3), the MC equations thus deserve study as generic amplitude equations in their own right. We observe that the long-wave amplitude f plays the role of a velocity-like variable in the direction of the pattern; since its spatial average is preserved by Eq. (2), by Galilean invariance we may assume f to have mean zero.

II. CHAOS-STABILIZED FRONTS

In describing properties of the MC equations (1)–(2), we emphasize the dynamics of the large-scale mode f , since the pattern amplitude A appears to be driven by f . We note that several aspects of the behavior for relatively small L have been previously described by Sakaguchi and Tanaka [12].

The snapshot of a solution for domain size $L = 51.2\pi$ shown in Fig. 1 is typical of the statistically stationary behavior

*Current address: School of Earth and Ocean Sciences, University of Victoria, Victoria, British Columbia, Canada V8W 3V6.

†ralf@sfu.ca

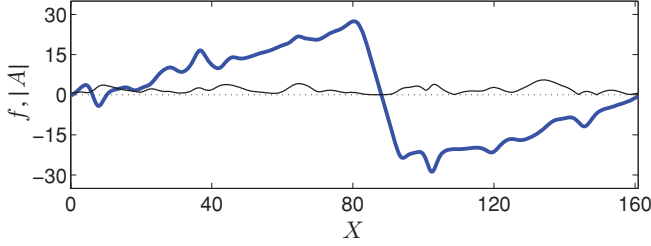


FIG. 1. (Color online) Snapshot at a fixed time $T_1 = 28,000$ of $f(X, T_1)$ (thick blue line) and $|A(X, T_1)|$ (thin black line) for a solution of Eqs. (1)–(2) with $L = 51.2\pi \approx 160.8$.

for “small” domains. The overall structure of f resembles a perturbed viscous shock, with f decreasing essentially linearly within the “front” region. Simultaneously, $|A|$ vanishes in the center of the front; Sakaguchi and Tanaka hence call this an “amplitude death” state [12]. The time evolution of a typical solution shown in Fig. 2 clearly shows the invariance of the front structure in f and the suppression of the roll amplitude A within the front region.

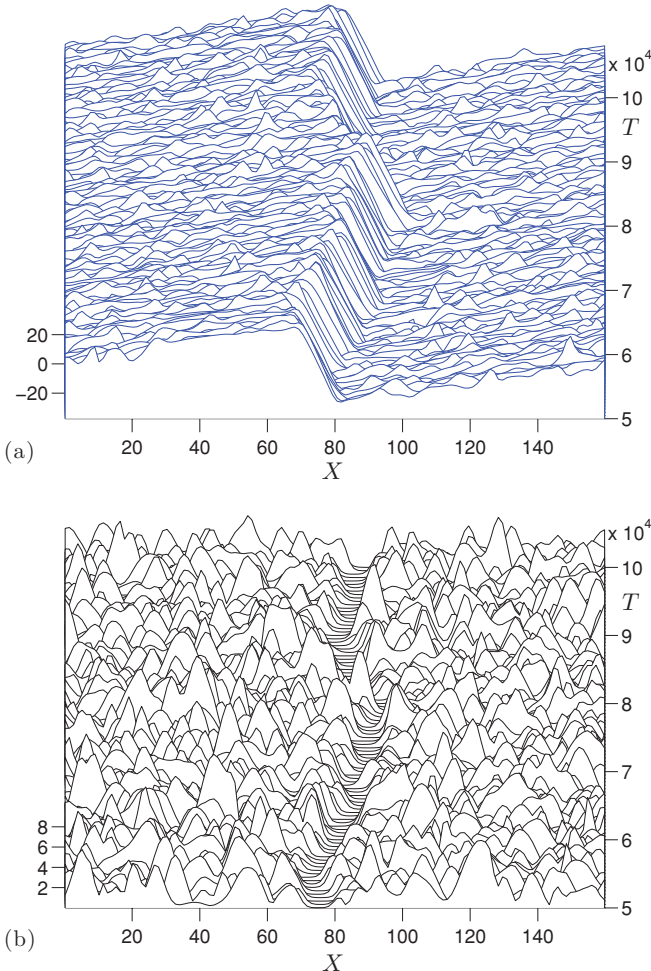


FIG. 2. (Color online) Space-time plots of long-time solutions (a) $f(X, T)$ and (b) $|A(X, T)|$ of the MC equations for $L = 51.2\pi$, and over a time interval of length 5×10^4 in T .

On the remainder of the domain, chaotic fluctuations in f [on $\mathcal{O}(1)$ timescales] are superposed on the approximately linear average positive slope and correlated (in space and time) with chaos in A . This coexistence of an ordered front (amplitude death state) and spatiotemporal chaos in spatially separate regions is robust on all domains $L \gtrsim L_0$ large enough to sustain the front [12].

The space-time plot indicates that the overall viscous shock profile in f is nonstationary but maintains its shape up to small fluctuations; that is, short-time averages¹ $\langle f(X, \cdot) \rangle_\tau$ are invariant up to translation. Denoting the averaged profile by $g(X) = g^{(L)}(X)$, where we center the front so $g(L/2) = 0$, $g_X(L/2) < 0$, and defining the front displacement $s(T)$ so that the instantaneous front position is $X_s(T) = L/2 + s(T)$, we may decompose the large-scale mode as $f(X, T) = g[X - s(T)] + \tilde{f}[X - s(T), T]$, where \tilde{f} denotes fluctuations about the mean profile. The unsteady dynamics in A and \tilde{f} are then essentially confined to the region where $g_X \geq 0$ and to the vicinity of the local extrema of g [see Fig. 3(c)].

To help clarify this unusual behavior, we observe that Eq. (2) for the large-scale mode f has the form of a conservation law [12],

$$f_T = -J_X, \quad \text{where} \quad J = -f_X + |A|^2. \quad (4)$$

Taking long-time averages, $\langle J \rangle_X = -\langle f_T \rangle = 0$, so in statistical equilibrium, the time-averaged flux J is uniform in X , $\langle J \rangle = \langle -f_X + |A|^2 \rangle \equiv \gamma$. Integrating over the domain and using periodicity, we find

$$\gamma = \gamma(L) = \frac{1}{L} \int_0^L \langle |A(X, \cdot)|^2 \rangle dX > 0. \quad (5)$$

Now for a stationary amplitude death domain, where $\langle |A|^2 \rangle = 0$, we have $\gamma = -\langle f_X \rangle$; this confirms that amplitude death can occur only where f is decreasing on average. [In fact, due to the apparent separation of time scales between the rapid fluctuations \tilde{f} , on $\mathcal{O}(1)$ times, and the slow overall drift of the mean profile $g(X)$, short-time averaging seems sufficient to conclude $\langle f_T \rangle_\tau \approx 0$, so that the mean midfront slope is $g_X(L/2) = -\gamma$.] By Eq. (5) the (averaged) slope $-\gamma$ of the large-scale mode f in the center of the amplitude death state thus seems to be globally determined, being balanced by the mean-square amplitude of the pattern mode A due to chaotic dynamics concentrated outside the front region.

Note that also $\gamma = \langle |A|^2 \rangle$ wherever $\langle f_X \rangle = 0$, relating the front slope to the fluctuations in A at extrema of the averaged profile. Indeed, in the absence of A , f satisfies a heat equation and thus by Eq. (4) flows away from local maxima and toward local minima, leading to spreading and dissipation of the front; the added forcing term in Eq. (2) when $|A|_X^2 \neq 0$ increases the flux J so as to maintain the averaged

¹Short-time averages $\langle f(X, \cdot) \rangle_\tau$ are taken over time intervals τ long relative to the $\mathcal{O}(1)$ timescales of the chaotic fluctuations, but short compared with front translations or transient coarsening (we use $\tau \gtrsim 40$).

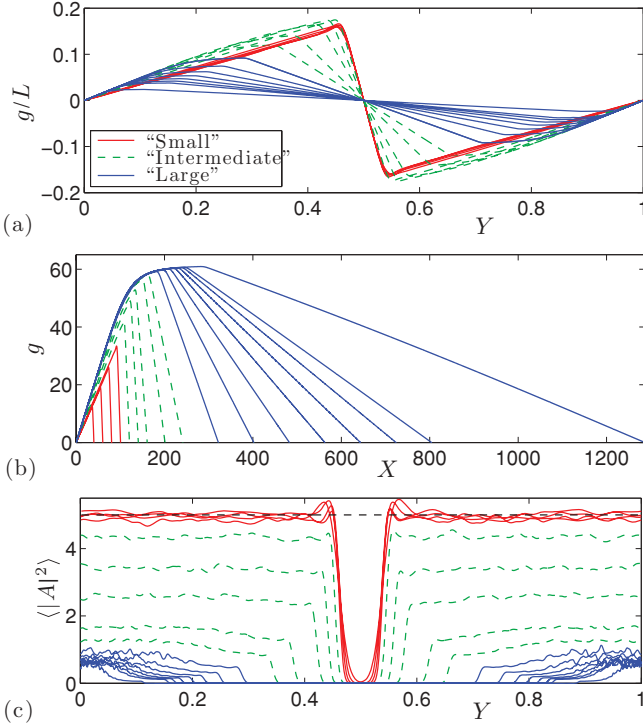


FIG. 3. (Color online) (a) and (b) Two representations of the long-time-averaged (centered) profile $g(X) = \langle f(X + s(\cdot), \cdot) \rangle$ of the large-scale mode f for various L : (a) scaled horizontally and vertically, $L^{-1}g(LY)$ for $Y = X/L \in [0, 1]$; (b) unscaled, half of the (odd) profile, $g(X)$ for $X \in [0, L/2]$. (c) Centered time-averaged pattern amplitude $\langle |A(LY, \cdot)|^2 \rangle$. Domain sizes are (“small”: gray, red online) $L = 25.6\pi, 38.4\pi, 51.2\pi, 64\pi$; (“intermediate”: green, dashed lines) $L = 76.8\pi, 89.6\pi, 102.4\pi, 128\pi, 153.6\pi$; and (“large”: black, blue online) $L = 204.8\pi, 256\pi, 307.2\pi, 358.4\pi, 409.6\pi, 460.8\pi, 512\pi$, and 819.2π . Averages were taken over time periods $T = 1 \times 10^5$ (small, intermediate) and 2×10^4 (large), with $\Delta T = 10$ between snapshots.

overall flux balance, thereby stabilizing the (averaged) local extrema. The stabilization mechanism in the MC equations thus appears to act globally,² with the chaotic dynamics being instrumental in sustaining the front (and amplitude death state); we denote the observed structures “chaos-stabilized fronts.”

[We remark that Eq. (1) does not contain the usual stabilizing GL cubic term, permitting Eqs. (1)–(2) to support a family of exponentially growing solutions $A(X, T) = A_0 e^T$, $f(X, T) = 0$; that is, the MC equations do not have a bounded global attractor. However, these growing solutions are dynamically unstable, in the sense that they are overtaken by faster-growing spatially varying perturbations [2]; and in our numerical simulations we have not observed such solutions.]

²Our findings are inconsistent with the local stability criterion (neglecting the sign of f_X) proposed in Ref. [12], that the amplitude death state is stable when the gradient of f is sufficiently large, $|f_X| > f_{0c}$ for $f_{0c} \approx 0.44$; for large L we find $\gamma \lesssim \mathcal{O}(1/L)$ and observe stable fronts, for instance, with $\gamma \lesssim 0.25$ for $L \gtrsim 1000$ [see Fig. 4(b)].

To investigate the behavior of the MC equations on spatially periodic domains systematically, we have numerically integrated Eqs. (1)–(2) using a pseudospectral method in space and an exponential time differencing (ETDRK4) scheme with step size $H = 0.02$. The domain length L , the only free parameter in the system, was chosen to be $L = 2\pi \times 64m/10$ for integers m ranging from 2 to 64; correspondingly, we used between 2^9 and 2^{14} Fourier modes. In computing time averages, we integrated until the system reached a statistically stationary single-front state, and then averaged over 10^3 – 10^4 snapshots separated typically by time intervals $\Delta T = 10$. All averaging was done within the frame of reference of the front; that is, we first determined the front displacement $s(T)$ and used it to align A and f so that the front was centered at $X = L/2$. In particular, the mean profiles were computed by $g(X) = \langle f(X + s(\cdot), \cdot) \rangle$.

III. AVERAGED PROFILES

As seen in Fig. 3, the averages of f and $|A|$ are, respectively, odd and even about $X = L/2$, recovering the reflection symmetry of the underlying PDEs (1)–(2). More interestingly, though, the time-averaged profiles $g(X)$ for $L \gtrsim L_0$ depend strongly on L , with the behavior falling into three distinct regimes.

For relatively “small” domains, $L_0 \lesssim L \lesssim L_1 \approx 220$, the scaled profiles in Fig. 3(a) approximately coincide, indicating a scaling form for g : For some fundamental shape function G , periodic on $[0, 1]$, we have $g(X) \approx LG(Y)$ (with $Y = X/L$). In this “small- L ” regime the scaling relation is highly accurate within the front [but is weakly violated outside it: the slope $\alpha = g_X(0)$ in the active region increases slowly with L ; see Fig. 4(a)]; in particular, the midpoint slope is independent of L , with $-\gamma = g_X(L/2) = G'(0.5) \approx -4.6$ (cf. Ref. [12]); see Fig. 4(b), where we have also numerically verified Eq. (5). We also find that the relative sizes of the front and chaotic regions

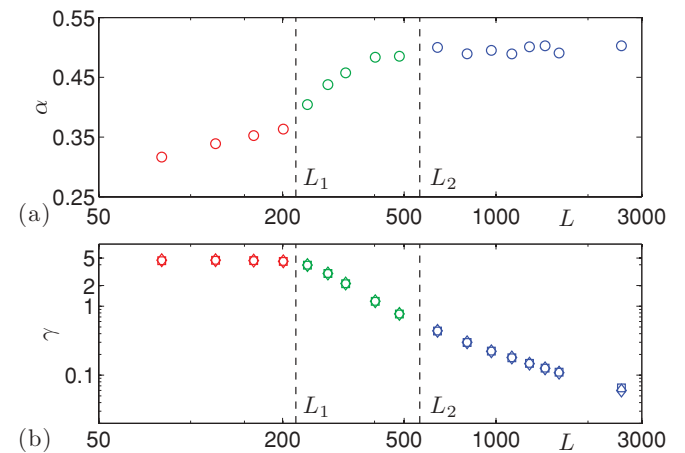


FIG. 4. (Color online) (a) Slope $\alpha = g_X(0)$ of averaged profile at midpoint of chaotic region. (b) Absolute value of midfront slope $\gamma = -g_X(L/2)$ (\square), shown with the mean-square average pattern amplitude $L^{-1} \int_0^L |A(X, \cdot)|^2 dX$ (\diamond), verifying Eq. (5). Lengths L and colors are as in Fig. 3; the vertical lines at $L_1 \approx 220$ and $L_2 \approx 560$ indicate approximate transitions between “small,” “intermediate,” and “large” regimes.

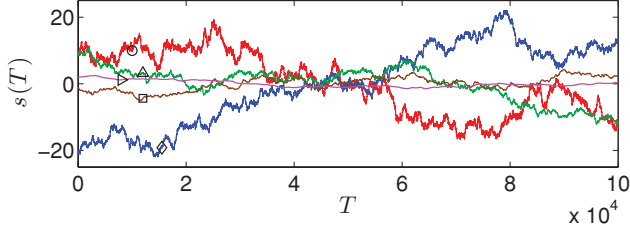


FIG. 5. (Color online) Representative trajectories of the front displacement $s(T)$ about $X = L/2$ for the “small” domains $L = 38.4\pi$ (red \circ) and 51.2π (blue \diamond), and “intermediate” sizes $L = 76.8\pi$ (green), 102.4π (brown \square), and 153.6π (magenta \triangleright).

remain fixed, with $\langle |A|^2 \rangle(X) \approx 5$ approximately constant and L -independent in the chaotic region [Fig. 3(c)]. For these “small” domain sizes, the front translates over long times (recall Fig. 2); interestingly, the statistics of the front motion appear consistent with a random walk [13], as suggested by the trajectories of $s(T)$ shown in Fig. 5.

The (approximate) scaling form for the time-averaged profile $g(X)$ observed for “small” domains breaks down for larger L . Instead, for domain sizes in an “intermediate” regime with lengths $L_1 \lesssim L \lesssim L_2 \approx 560$, the amplitude of g begins to level off, the front becomes wider and less steep, and chaotic fluctuations of A and f decrease in amplitude (see Figs. 3–4). Furthermore, the variance of the front displacement $s(T)$ decreases strongly with L , until the translation becomes imperceptible (Fig. 5).

This behavior is transitional to that of “large” domains $L \gtrsim L_2 \approx 560$. In this regime the front is stationary, $s(T) \equiv 0$; the amplitude of $g(X)$ saturates at $\max g \approx 62$, as does the maximum slope in the chaotic region, $\alpha = g_X(0) \approx 0.5$. Indeed, Fig. 3(b) shows that the mean profile $g(X)$ near $X = 0$ becomes invariant with increasing L ; this saturation of the profile indicates to us that we have reached the large- L asymptotic regime of (1)–(2). Since the width of the amplitude death region continues to grow with L , while the height is bounded, the front slope $-\gamma$ decays with L , and hence so does the amplitude of the fluctuations in A : For large L the spatially confined chaotic dynamics superposed on the mean profile are strongly suppressed.

IV. TRANSIENT BEHAVIOR

The strong L -dependence of the properties of the MC equations, within identifiable domain size regimes, is apparent also in the transient approach to the long-time statistically stationary state, as summarized in the time evolution of $w(T) = [L^{-1} \int_0^L f(X, T)^2 dX]^{1/2}$ —analogous to an interface width in the context of surface growth—as in Fig. 6. The snapshots from a typical time evolution for a “large” domain in Fig. 7 demonstrate an extended coarsening period followed by a remarkable collapse to a single front.

From small random data, initial growth rapidly establishes a sawtooth pattern in f , as in Fig. 7(a): a concatenation of structures, of varying widths and corresponding heights, locally reminiscent of the statistically stationary states in “small” domains (see Fig. 8). Once this metastable state

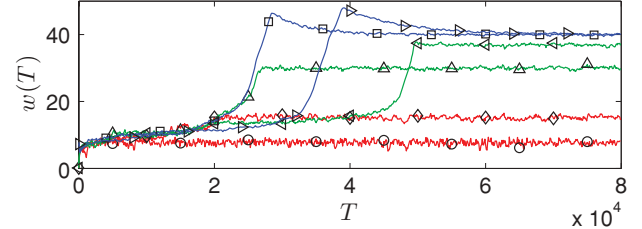


FIG. 6. (Color online) Evolution of $w(T) = [L^{-1} \int_0^L f(X, T)^2 dX]^{1/2}$ for the “small” domains (red) $L = 25.6\pi$ (\circ) and 51.2π (\diamond); “intermediate” domains (green) $L = 89.6\pi$ (\triangle) and 128π (\triangleleft); and “large” domains (blue) $L = 256\pi$ (\square) and 307.2π (\triangleright), computed to $T = 8 \times 10^4$.

of multiple Burgers-like viscous shocks with superposed chaotic fluctuations is established, a slow coarsening process ensues: Front structures grow and merge with adjacent fronts, leading to a gradual increase of length scales and of $w(T)$ [Fig. 7(a)–7(d)].

For “small” domains, for which the long-time state has the (approximate) scaling form G on average, this coarsening concludes once there is a single front. However, for “intermediate” and “large” domains, the gradual growth of $w(T)$ through coarsening is followed by a “jump” in $w(T)$ (see Fig. 6). The initiation times for these jumps are not monotonic in L and are widely distributed for each L for varying initial conditions (we have observed them to occur throughout the

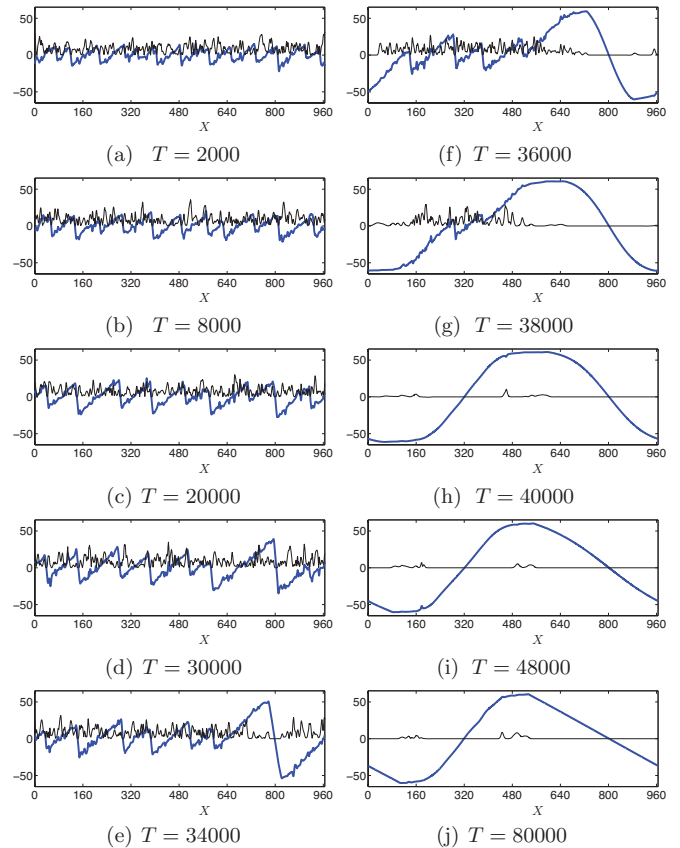


FIG. 7. (Color online) Snapshots of f (thick blue line) and $|A|$ (black; for clarity we plot $5|A|$) showing coarsening and collapse to a single front for $L = 307.2\pi \approx 964.8$.

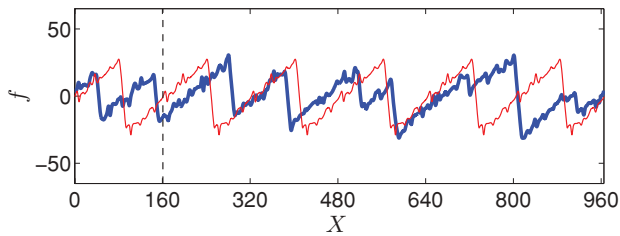


FIG. 8. (Color online) Large-scale mode f at $T = 28,000$ for the “large” domain $L = 307.2\pi$ (thick blue line) with, for comparison, six (red) copies of the $L = 51.2\pi$ profile from Fig. 1.

range $T \approx 2-8 \times 10^4$), while the growth rate of $w(T)$ during the jump appears to be L -independent [13]. This behavior of $w(T)$ reflects qualitative changes in the profile $f(X, T)$, as seen in Fig. 7(d)–7(h). Specifically, having (presumably) exceeded a critical size, one of the front structures begins to dominate and then grows relatively rapidly by engulfing its neighbors until a state with an L -dependent single front is attained.

Finally, for “large” domains, $w(T)$ overshoots its asymptotic value (Fig. 6), since following the collapse to a single front, the profile of f is not initially linear in the amplitude death region; f subsequently undergoes slow diffusive relaxation [by Eq. (2) with $|A| = 0$] to the time-asymptotic linear front profile [Fig. 7(h)–7(j)].

V. DISCUSSION

The Matthews-Cox equations (1)–(2), the leading-order amplitude equations for finite-wavelength pattern formation with Galilean invariance, form a relatively simple deterministic

system displaying a remarkable richness of behaviors: a domain size-dependent coexistence of ordered and chaotic states, with fronts stabilized by spatiotemporal chaos, attained after a multiple-stage transient including slow coarsening and rapid collapse to the single-front time-asymptotic state. In light of our observations, we expect that this system provides interesting theoretical challenges.

The structure of the MC equations is reminiscent of that of other well-known systems. For instance, viewing Eq. (2) as a heat equation for f with (chaotic, spatially nonuniform) forcing, using the heat kernel to express f as a quadratic functional of A and substituting, the $-ifA$ coupling term in Eq. (1) acts as a nonlocal cubic stabilizing term in a Ginzburg-Landau-type equation.

Alternatively, in light of the viscous shocklike behavior in f , it may be fruitful to view Eq. (2) as a generalized viscous Burgers’ equation with a nonlocal forcing term: In this case, the fronts in f are driven not by the usual ff_X Burgers’ nonlinearity (which appears at higher order in the MC scaling [2,11]), but rather by gradients in $|A|^2$, where A is determined, for a given $f(X, T)$, via the linear, nonconstant-coefficient PDE (1). Such considerations may facilitate a theoretical understanding of the unusual behavior we have described in the MC equations.

ACKNOWLEDGMENTS

We thank the IRMACS Centre at Simon Fraser University for providing a productive research environment and David Muraki, Richard Kollár, and the anonymous referees for helpful discussions and suggestions. This work was partially supported by NSERC.

-
- [1] M. Cross and P. Hohenberg, *Rev. Mod. Phys.* **65**, 851 (1993).
 - [2] P. C. Matthews and S. M. Cox, *Phys. Rev. E* **62**, R1473 (2000).
 - [3] I. A. Beresnev and V. N. Nikolaevskiy, *Physica D* **66**, 1 (1993).
 - [4] H. Fujisaka and T. Yamada, *Prog. Theor. Phys.* **106**, 315 (2001).
 - [5] D. Tanaka, *Phys. Rev. E* **70**, 015202(R) (2004).
 - [6] S. M. Cox and P. C. Matthews, *Phys. Rev. E* **76**, 056202 (2007).
 - [7] M. I. Tribel’skiĭ, *Usp. Fiz. Nauk* **167**, 167 (1997).
 - [8] M. I. Tribelsky and M. G. Velarde, *Phys. Rev. E* **54**, 4973 (1996).
 - [9] M. I. Tribelsky and K. Tsuboi, *Phys. Rev. Lett.* **76**, 1631 (1996).
 - [10] D. Tanaka, *Phys. Rev. E* **71**, 025203(R) (2005).
 - [11] R. W. Wittenberg and K.-F. Poon, *Phys. Rev. E* **79**, 056225 (2009).
 - [12] H. Sakaguchi and D. Tanaka, *Phys. Rev. E* **76**, 025201(R) (2007).
 - [13] K.-F. Poon, Ph.D. thesis, Simon Fraser University, 2009.